Near-infrared IOTA interferometry of the symbiotic star CH Cyg

K.-H. Hofmann[a], U. Beckmann[a], J. Berger[b], T. Blöcker[a], M.K. Brewer[c], M. Lacasse[b], V. Malanushenko[e], R. Millan-Gabet[b], J. Monnier[b], K. Ohnaka[a], E. Pedretti[b], D. Schertl[a], P. Schloerb[c], M. Scholz[f], W. Traub[b], G. Weigelt[a], B. Yudin[d]

[a]Max-Planck-Institut für Radioastronomie, 53121 Bonn, Germany
[b]Harvard-Smithsonian Center for Astrophysics, Cambridge, MA 02138, USA
[c]Physics and Astronomy Dept., Univ. Massachusetts, Amherst, MA 01003, USA
[d]Sternberg Astronomical Institute, 119899 Moscow, Russia
[e]Crimean Astrophysical Observatory, 98409 Crimea, Ukraine
[f]Institut für Theoretische Astrophysik der Universität Heidelberg, 69121 Heidelberg, Germany, and Institute of Astronomy, School of Physics, University of Sydney NSW 2006, Australia

ABSTRACT

We present observations of the symbiotic star CH Cyg with a new JHK-band beam combiner mounted to the IOTA interferometer[1]. The new beam combiner consists of an anamorphic cylindrical lens system and a grism, and allows the *simultaneous* recording of spectrally dispersed J-, H- and K-band Michelson interferograms. The observations of CH Cyg were conducted on 5, 6, 8 and 11 June 2001 using baselines of 17 m to 25 m. From the interferograms of CH Cyg, J-, H-, and K-band visibility functions can be determined. Uniform-disk fits to the visibilities give, e.g., stellar diameters of (7.8 ± 0.6) mas and (8.7 ± 0.8) mas in H and K, respectively. Angular stellar filter radii and Rosseland radii are derived from the measured visibilities by fitting theoretical center-to-limb intensity variations (CLVs) of Mira star models[2,3]. The available HIPPARCOS parallax of CH Cyg allows us to determine linear radii. For example, on the basis of the K-band visibility, Rosseland radii in the range of 214 to 243 $R_\odot$ can be derived utilizing CLVs of different fundamental mode Mira models as fit functions. These radii agree well within the error bars with the corresponding theoretical model Rosseland radii of 230 to 282 $R_\odot$. Models of first overtone pulsators are not in good agreement with the observations. The wavelength dependence of the stellar diameter can be well studied by using visibility ratios $V(\lambda_1)/V(\lambda_2)$ since ratios of visibilities of different spectral channels can be measured with higher precision than absolute visibilities. We found that the 2.03 μm uniform disk diameter of CH Cyg is ∼1.1 times larger than the 2.15 μm and 2.26 μm uniform-disk diameter.

Keywords: interferometry, symbiotic stars, near-infrared

1. INTRODUCTION

Symbiotic stars are close binary systems consisting of a cool red giant and a hot blue star. Interaction of both components can lead to accretion phenomena and highly variable lightcurves. CH Cyg is one of the best studied members of this class of stars. It is a luminous triple symbiotic system with a very complicated photometric and spectroscopic behaviour[4]. The red giant's diameter is one crucial parameter for the investigation of such systems and therefore high-resolution interferometric measurements may provide important information[1]. Previous interferometric K-band observations of CH Cyg carried out by Dyck et al.[5] (1996 Oct. 7) yielded a uniform disk diameter of 10.4 ± 0.6 mas.

The size of a star can be derived by observing the brightness distribution on its stellar disk. For the interpretation detailed dynamic atmosphere models have to be taken into account which predict, for instance, center-to-limb intensity variations and corresponding visibilities[6]. By comparing the observations with such

models, fundamental stellar parameters can be derived. It is well known that the stellar diameter may vary with wavelength[7]. Accordingly, simultaneous measurements in different spectral bands greatly constrain the analysis.

2. OBSERVATIONS AND UNIFORM-DISK FITS

CH Cyg was observed with the IOTA interferometer using a new JHK beam combiner developed at the Max-Planck Institute for Radioastronomy. This NIR beam combiner consists of an anamorphic lens system and a grism, and is similar to the dispersed-fringe instruments used at the I2T/GI2T interferometer in the optical wavelength range[8]. A full description will be given elsewhere. The observations were carried out on June 5, 6, 8 and 11, 2001 with baselines between 17 m and 25 m. The observational parameters are given in Table 1. The raw visibilities of each spectral channel and each baseline were derived by evaluating the power spectra of the interferograms (determination of the ratio of off-axis and central peak). The calibrated visibilities were reconstructed from the raw visibilities of the object and the raw visibilities of reference stars. Figure 1 (see also Table 1) shows the calibrated H and K visibilities and their uniform-disk (UD) fits which yield H- and K-band UD stellar diameters of 7.8 mas ± 0.6 mas and 8.7 mas ± 0.8 mas, respectively (along position angle $\sim 0^o$).

Table 1. IOTA observations of CH Cyg. B_p is the projected baseline, N denotes the total number of recorded interferograms, and V_K and V_H are the measured visibilities in the K and H, respectively.

Date	B_p [m]	N	V_K	V_H	Ref. stars
2001 June 05/06	20.08	12200	0.81±0.05	0.74±0.06	d Cyg, HR 7924
2001 June 08	24.55	11000	0.73±0.05	0.66±0.05	d Cyg, HR 7924
2001 June 11	17.37	11200	0.84±0.07	0.81±0.08	d Cyg, e Dra

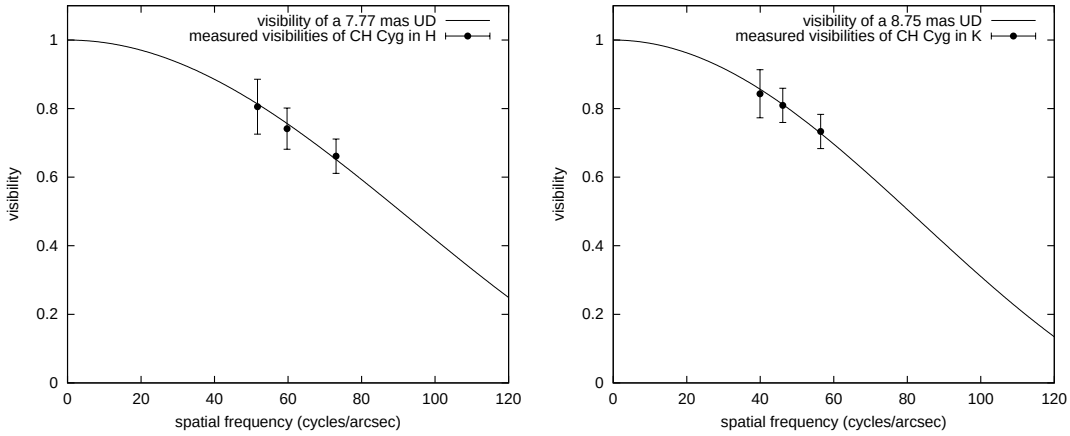

Figure 1. Uniform-disk (UD) fits to the visibilities of CH Cyg measured in the H (left) and K band (right).

3. COMPARISON OF THE OBSERVATION WITH MIRA STAR MODELS

3.1. Mira star models

Angular diameters can be derived from the observations by fitting the measured visibilities with theoretical center-to-limb intensity variations of Mira star models (Bessel, Scholz & Wood[2]; Hofmann, Scholz & Wood[3]). These models were developed as possible representations of the prototype Mira variable o Ceti, and hence have periods P very close to the 332 day period of o Ceti; they differ in pulsation mode (fundamental, f, or first overtone, o), assumed mass M and luminosity L, and in modelling assumptions. Table 2 lists the properties

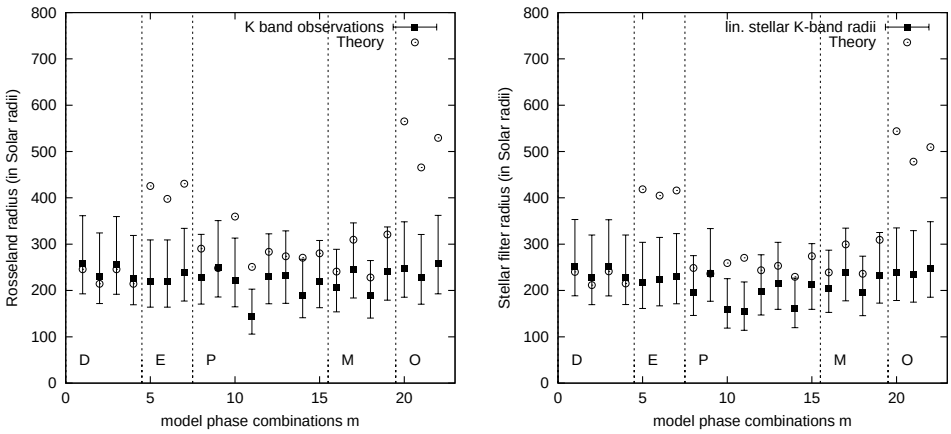

Figure 2. Comparison of derived CH Cyg radii (filled squares) with theoretical model radii (open circles). Left: linear Rosseland radii $R_{\rm m}$ for all 22 model-phase combinations m. Different values of m correspond to different phases or cycles (see Ref. 9). Right: linear stellar K-band radii for all 22 model-phase combinations m.

of the model series used ($R_{\rm p}$ = Rosseland radius of the non-pulsating "parent" star of the Mira variable[2,3]; $T_{\rm eff}$ = effective temperature). These models predict monochromatic radii R_λ (radius at which the optical depth equals unity, i.e. $\tau_\lambda = 1$), Rosseland radii R (radius at which the Rosseland optical depth equals unity, i.e. $\tau_{\rm Ross} = 1$), and stellar filter radii $R_{\rm f}$ ($= \int R_\lambda\, I_\lambda\, {\rm f}_\lambda\, d\lambda \,/\, \int I_\lambda\, {\rm f}_\lambda\, d\lambda$, with $\rm f_\lambda$ being the filter transmission, R_λ the monochromatic radius, and I_λ the intensity spectrum) at different pulsational phases and cycles. These predictions are compared with our measurements in the following section.

Table 2. Mira model series (see text). For more details we refer to Ref. (2,3).

Series	Mode	P(d)	$M/M_\odot$	$L/L_\odot$	$R_{\rm p}/R_\odot$	$T_{\rm eff}$/K
D	f	330	1.0	3470	236	2900
E	o	328	1.0	6310	366	2700
P	f	332	1.0	3470	241	2860
M	f	332	1.2	3470	260	2750
O	o	320	2.0	5830	503	2250

3.2. Derived angular stellar filter radii, angular Rosseland radius and linear radii

The derived angular stellar filter radii $R^a_{\rm K,m}$ and $R^a_{\rm H,m}$ (m: model-phase combinations) were determined by least-squares fits of the model[2,3] CLV visibilities to the measured visibilities. From the obtained stellar filter radii and the theoretical ratios of $R/R_{\rm p}$ to $R_{\rm K}/R_{\rm p}$ and $R_{\rm H}/R_{\rm p}$, respectively, predicted by the above Mira star models (see Table 3 in Ref. 9), the angular Rosseland radii $R^a_{\rm m}$ can be derived.

Linear stellar filter radii ($R_{\rm K,m}$, $R_{\rm H,m}$), and linear Rosseland radii ($R_{\rm m}$) of CH Cyg were determined from the derived angular stellar filter radii ($R^a_{\rm K,m}$, $R^a_{\rm H,m}$) and Rosseland radii ($R^a_{\rm m}$) using the CH Cyg HIPPARCOS parallax of 3.73 ± 0.85 mas[10,11]. Fig. 2 shows the obtained linear Rosseland radii $R_{\rm m}$ (derived from the K-band visibilities) and the stellar filter radii $R_{\rm K,m}$ for all model-phase combinations m. The theoretical Rosseland radii of the fundamental mode D, M and P model series are at almost all available phases close to the Rosseland radii of CH Cyg derived from the observations. On the other hand, the first-overtone models E and O give Rosseland radii which are too large. Table 3 compares the theoretical D-, P- and M-model Rosseland radii with the derived linear Rosseland radii determined from the K-band visibilities and the D-, P- and M-model CLVs. The phase-averaged derived linear Rosseland radii are averages over all pulsational phases. Table 3 shows that

Table 3. Comparison of the derived linear Rosseland radii of CH Cyg with the corresponding theoretical Rosseland radii. For comparison, the linear UD K-band radius is 251^{+100}_{-63} $R_\odot$.

Model	Phase-averaged linear Rosseland radius ($R_\odot$) derived from the K-band obs.	Theoretical linear Rosseland radius ($R_\odot$)
D	243^{+98}_{-62}	230
P	214^{+87}_{-55}	282
M	220^{+89}_{-56}	275

there is good agreement within the error bars between the measured uniform-disk radius, the derived Rosseland radii, and the theoretical Rosseland radii. We note that the HIPPARCOS parallax error contributes most to the given total error bars.

Iijima[4] detected eclipsing phenomena of the inner binary of the CH Cyg system with a period of 756 d by spectrophotometric observations. From the duration of the hot component's eclipse by the red giant, a radius of 288 $R_\odot$ was estimated for the red giant slightly larger than the one inferred from our interferometric measurements.

4. DIAMETER RATIOS $\frac{D(\lambda_1)}{D(\lambda_2)}$ DERIVED FROM VISIBILITY RATIOS $\frac{V(\lambda_1)}{V(\lambda_2)}$

Our JHK interferograms allow us to derive from each interferogram the visibilities of many different spectral channels in the wavelength range of 1-2.3 μm. We use these visibilities to determine the diameter ratios $D(\lambda_1)/D(\lambda_2)$ and compare these observed ratios with theoretical model ratios[12].

For this goal we have divided our K-band interferograms into three wavelength bins of approximately 0.1 μm width and derived the visibility ratios $V_{2.03\,\mu m}/V_{2.26\,\mu m}$, $V_{2.15\,\mu m}/V_{2.26\,\mu m}$ and $V_{2.03\,\mu m}/V_{2.15\,\mu m}$. From these visibility ratios we can derive diameter ratios which show that the diameter of CH Cyg is larger at 2.03 μm than at 2.15 μm or 2.26 μm. If the CH Cyg visibilities $V_{2.03\mu m}$, $V_{2.15\mu m}$, and $V_{2.26\mu m}$ are fitted by uniform-disks, diameter ratios of $D_{2.03\mu m}/D_{2.26\mu m} = 1.11$, $D_{2.03\mu m}/D_{2.15\mu m} = 1.12$, and $D_{2.15\mu m}/D_{2.26\mu m} = 0.99$ are obtained. These ratios agree with both the predicted theoretical diameter ratios[12] and observations presented in Ref. 13. A full account of the above studies (comparison with Mira models at JHK, wavelength dependence of the diameter in JHK, derivation of effective temperature from JHK radii and coeval $UBVJHKLM$ photometry) will be presented in Ref. 14.

5. REFERENCES

1. W.A. Traub, SPIE 3350, 848, 1998
2. M.S. Bessell, M. Scholz, M., and P.R. Wood 1996, *A&A*, 307, 481
3. K.-H. Hofmann, M. Scholz, and P.R. Wood 1998, *A&A*, 339, 846
4. T. Iijima, 1998, *MNRAS 297*, 77
5. H.M. Dyck, G.T. van Belle, R.R. Thompson 1998, *AJ*, 116, 981
6. M. Scholz, 2001, *MNRAS 321*, 347
7. A. Labeyrie, L. Koechlin, D. Bonneau, A. Blazit, R. Foy. 1977, *ApJ* 218, L75
8. A. Labeyrie, G. Schumacher, M. Dugue, C. Thom, P. Bourlon, F. Foy, D. Bonneau, R. Foy 1986, *A&A* 162, 359
9. K.-H. Hofmann, U. Beckmann, T. Blöcker, et al. 2001, *New Astronomy*, 7, 9-20
10. ESA 1997, The Hipparcos & Tycho Catalog, ESA SP-1200, Noordwijk: ESA
11. F. Van Leeuwen, M.W. Feast, P.A. Whitelock, and B. Yudin 1997, *MNRAS*, 287, 955
12. A.P. Jacob and M. Scholz "Effects of molecular contamination of IR near-continuum bandpasses on measurements of M-type Mira diameters", MNRAS, in press
13. R.R. Thompson, M.J. Creech-Eakman and G.T. van Belle "Multi-epoch interferometric study of Mira variables I. Narrowband diameters of RZ Peg and S Lac", ApJ, in press
14. K.-H. Hofmann et al., 2002, "Near-infrared IOTA interferometry of the symbiotic star CH Cyg", in prep.